EXTREME GROUND MOTION RECORDED IN THE NEAR-SOURCE REGION OF UNDERGROUND NUCLEAR EXPLOSIONS

Bill Foxall

Lawrence Livermore National Laboratory

Introduction

Free-field recordings of underground nuclear explosions constitute a unique data set within the near-source region of seismic events ranging in magnitude from M3 to M6.5. The term "free-field" in this context refers to recordings from instruments emplaced in boreholes or tunnel walls such that the initial portions of the records (~0.1 to 1 second) do not contain effects resulting from reflections at the free surface. In addition to the free-field instruments deployed to record ground motions from selected underground nuclear explosions at the Nevada Test Site (NTS) and elsewhere, surface arrays were routinely deployed to record surface accelerations and velocities from underground nuclear tests conducted at NTS.

Underground explosions are quite different from earthquakes in that they are compressional rather than shear seismic sources, have a much higher energy density, and are detonated much closer to the surface - generally on the order of 1 km or less - than typical earthquake focal depths. The loading and failure mechanisms in the surrounding materials are therefore fundamentally different. However, there appears to be sufficient similarity in the damage and subsequent attenuation mechanisms produced by the two types of sources that it is likely that free-field recordings can provide important information to characterize highly non-linear energy dissipation mechanisms in the immediate source vicinity that limit extreme ground motions, and the transition through weak non-linearity to elastic wave propagation. The data also hold the potential of constraining the mechanical properties of materials analogous to those at Yucca Mountain under high strain loading. Furthermore, both free-field and surface recordings are a rich source of information on near-surface spall produced by explosions, which can be used to calibrate field observations that J. Brune has proposed as a potential means of placing limits on ground motions from earthquakes.

In this paper we provide an overview of the types of data recorded during the U.S. underground nuclear testing program and their availability, and briefly discuss potential uses of the data in investigating the limits on ground motions generated by earthquakes.

Instrument Arrays

The vast majority of the U.S. underground nuclear tests carried out between the mid-1950s and the end of testing in 1992 took place within three main areas at NTS, Yucca Flat, Pahute Mesa and Rainier Mesa. Detonation points of tests under Yucca Flat were in various tuff units or in the thick overlying alluvium section. Tests under Pahute Mesa and Rainier Mesa were detonated in tuffs, and were recorded on tuff and/or in thin

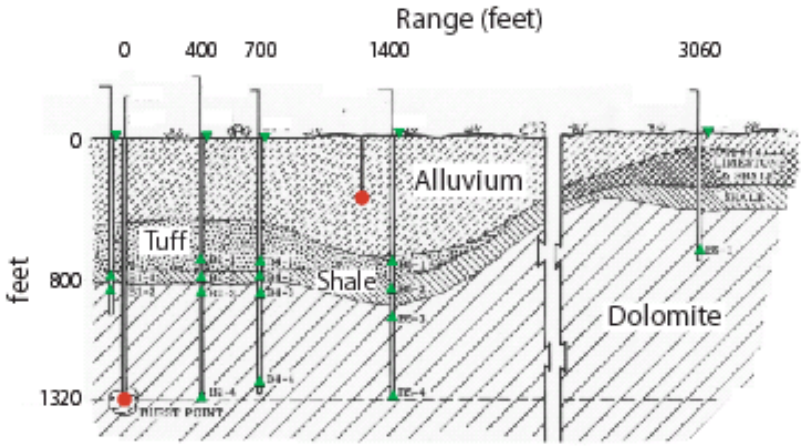

***Figure 1**: Surface and subsurface arrays (green) deployed for the HANDCAR_MUDPACK shots (red)*

superficial alluvium layers. The mechanical properties of shot point tuffs vary over a wide range, but include densely welded materials such as the Rainier Mesa member analogous to materials at repository depth at Yucca Mountain. Elaborate free-field and surface arrays of accelerometers and velocity sensors were deployed for several of the earlier (pre 1974) events conducted as weapons tests or as part of the Plowshare program (peaceful uses), or for non-proliferation experiments. For example, Figure 1 shows the array deployed for the 1964 HANDCAR-MUDPACK events. A more typical layout consisted of a string of accelerometers and/or velocity sensors deployed in a single borehole offset 10-30 m from the device emplacement hole, as shown in Figure 2. Lawrence Livermore National Laboratory (LLNL), for example, deployed such arrays on average once per year from 1978 onwards with the specific objective of calibrating dynamic models of wave propagation and material response conducted for containment purposes. The surface arrays routinely deployed by LLNL, LANL and Sandia (SNL) generally recorded strong ground motions within surface ranges ~1 km or less from surface ground zero, but extended to regional distances for certain special studies.

Data Availability

We have compiled a spread sheet of events for which we know free-field and/or surface ground motion exist. These include tests carried out by all agencies involved in the test program, including LLNL, LANL, and the Department of Defense (DOD). Most of the ground motion data are held by LLNL, LANL and SNL. Of the 381 events presently in the spread sheet, 169 have free-field data, 164 surface data, and 44 ground motion data from containment plugs in the emplacement hole. The LLNL containment program archive includes CDs of digital ground motion data for 189 NTS events between 1977 and 1992. LANL maintain a computerized data base that contains ground motion data for about 150 NTS events, including digitized analog data (App, 1994). The waveform data in both of these archives are unclassified and are available as ASCII or LLNL Seismic Analysis Code (SAC) files. (The yields of most of the tests remain classified.) In addition to the waveforms themselves, instrument calibrations are included in the archives, at least for the mid-1970s onwards. *In situ* geologic and material property data routinely compiled from the logs for every test emplacement hole are available either as printed reports or computer files. Material properties routinely compiled include P-wave velocity, bulk density and porosity, and water saturations for each lithologic unit. Other material property data were determined for specific units from laboratory tests. SNL are

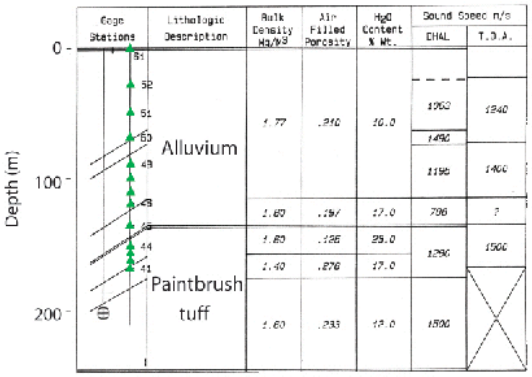

***Figure 2**: PERA vertical array (green)*

in the process of compiling a data base for 17 Rainier Mesa tunnel shots, which includes raw ground motion waveforms in ASCII format and associated calibration and other metadata. We have also located an archive of paper analog records at the DOE Nevada Operations Office in Las Vegas. These are presumably from early tests, but we have not yet examined the record catalogs in detail.

Overview of the Explosion Source

In order to describe the characteristics of free-field motion recorded in the near-source region, we first provide a brief overview of the explosion source. Figure 3 shows a generalized cartoon of the near-source region within an homogeneous half-space following a nuclear explosion. The rapidly expanding high temperature, high pressure bubble of gas (vaporized rock) created by the detonation creates a shock wave that first melts and then pulverizes the rock immediately surrounding the detonation point to create a cavity, radius R_c. At a short distance (less than the final cavity radius) from the detonation, the shock wave separates into an elastic precursor traveling at the P-wave speed of the undisturbed medium and the peak pressure pulse that propagates at a subsonic plastic wave speed. The peak stress of the shock wave as it propagates beyond the final cavity radius exceeds the yield shear stress of the rock and creates a zone of macroscopic damage out to a distance of about three cavity radii.

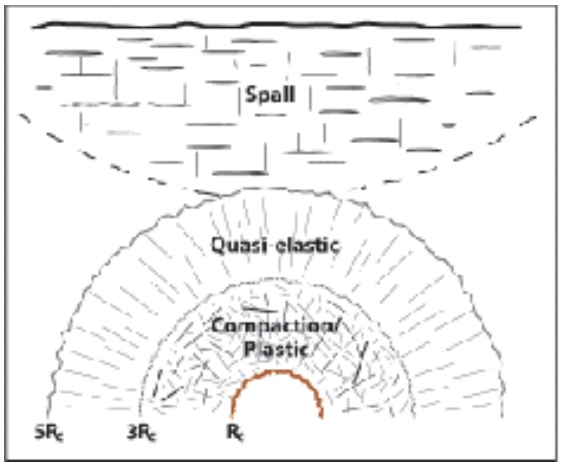

***Figure 3**: Explosion source*

The principal stresses (one radial, two tangential) within this zone are all compressive, and the predominant damage modes are pore compaction and collapse, and shear failure accompanied by dilatation. Damage and plastic yielding within the compaction zone rapidly attenuate the plastic wave such that the peak pressure falls below the yield stress and the tangential principal stresses become tensile on reaching the boundary of the zone, resulting in relatively minor tensile failure out to about five cavity radii. Within this zone the peak stress (main wave) propagates at the elastic P-wave speed but it attenuates quasi-elastically. Beyond this wave propagation is essentially elastic, but with minor non-linear behavior at ~10^{-6} strain. At about the time the shock wave has traversed the compaction zone the cavity wall

rebounds, followed by re-expansion and re-compaction and, finally, damped oscillations. These pulses propagate outwards to become later arriving peaks of an elastically propagating wave train beyond the quasi-elastic zone. When the main compressional peak reaches the free surface it is reflected as a tensional wave front that exceeds the tensional strength of the material, resulting in tensional failure, or spall, down to some depth such that near-surface layers actually detach and go ballistic. Table 1 summarizes empirical scaling of magnitude (m_b) and R_c and normal depth of burial with explosive yield, W, in kilotons.

Ground Motion Characteristics

To illustrate some of the general characteristics of near-source waveforms recorded by free-field arrays we summarize the analysis by Terhune and Heusinkveld (1983) of data recorded on the PERA array shown in Figure 2 and on similar vertical arrays for events NORBO, KARAB and TILCI. All of these tests were conducted under Yucca Flat. The first three were detonated in tuff, and TILCI, in alluvium. Figure 4a shows travel time curves for the main (peak velocity) wave for PERA (P), NORBO (N) and TILCI (T), and for the elastic precursor for KARAB (X); the detonation depths are indicated on the figure. Close to the source, the main waves propagate at subsonic (plastic) speeds before abruptly accelerating to elastic P-wave speeds similar to the speed of the elastic precursor from X. This transition defines the sharp boundary between the compaction and quasi-static zones (Figure 3), which Terhune and Heusinkveld show is also well defined by the limits of residual volumetric strain derived from the velocity data. Figure 4b shows peak velocity as a function of slant range (normalized to PERA) for events P, N and T. Out to a normalized range of about 80 m, again corresponding to the perimeter of the compaction zone, the peak velocity attenuates rapidly at ~R^{-3}, indicative of strong energy dissipation by pore compaction and plastic yielding. At the perimeter of the zone, the attenuation rate abruptly changes to ~R^{-1}, indicating quasi-elastic behavior. Note that the transitions in both velocity and attenuation rate are clearly defined by the data.

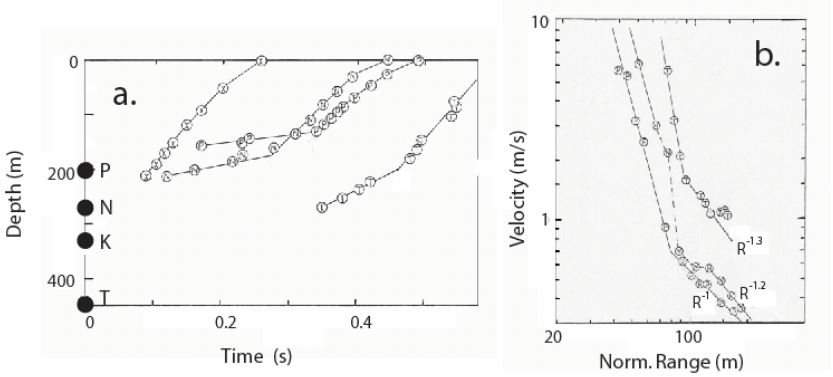

***Figure 4**: Travel time (**a**) and attenuation (**b**) curves*

Figure 5 shows the velocity waveforms recorded on the four sensors closest to shot NORBO [yield < 20 kt (DOE, 2000)], within the compaction zone (Figure 3). The waveforms are time-shifted to the first (elastic precursor) arrival time at one sensor, and amplitudes V_i are normalized such that $V_i' = V_i(R_i/R_0)^{\alpha}$, where R_i and R_0 are the slant ranges to sensor *i* and the reference sensor, respectively, and α is the average of the attenuation rates of the elastic precursor and the main wave across the four sensors. The first, compaction, pulse comprises the elastic precursor (PC) and the peak (main) velocity wave (PW), followed by the rebound (negative) and recompaction

(positive) pulses and the damped oscillations. The entire wave train propagates in-phase across the zone, each of the pulses having a constant duration. The compaction pulse attenuates very rapidly across the zone, but the later pulses attenuate at the same rate as the elastic precursor, suggesting quasi-elastic behavior within the compaction zone after the main compaction pulse has passed. Figure 6 shows the PERA [yield < 20 kt (DOE, 2000)] waveforms recorded just outside the compaction zone, where the pulses that developed in the compaction zone are still clearly defined and propagate in-phase at the P-wave speed. The entire wave train attenuates at the same rate as the precursor, so that the overall behavior is quasi-elastic. Figures 5 and 6 illustrate the general quality of the data recorded on the free-field arrays. We chose these examples because they clearly show the near-source phenomenology. More generally, however, the waveforms are complicated by refractions, reflections and wave conversions from lithological boundaries, which often have strong impedance contrasts in the highly stratified lithologies at NTS. Figure 6 shows a typical surface accelerogram recorded at a slant range of 1.1 km. The main wave peak acceleration at about 0.5 sec is almost 5g. This is followed by spall onset at about 0.6 sec, and ballistic free-fall (-1g) followed by the large slap-down peak at 0.9 sec.

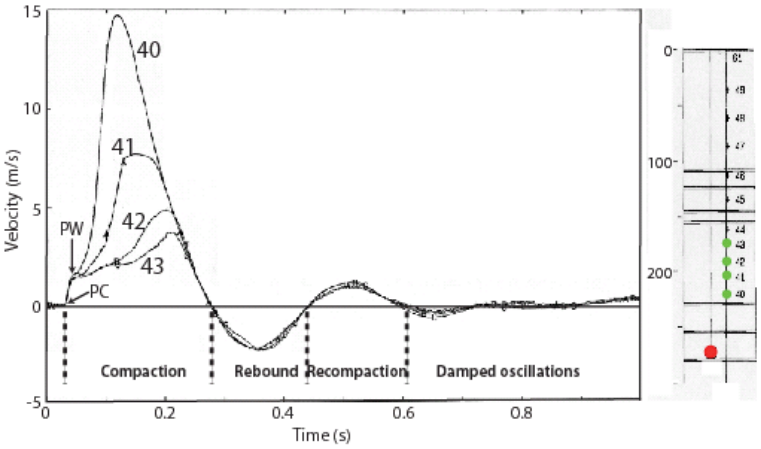

***Figure 5**: Velocity time histories for four sensors (green) within the compaction zone of event NORBO (red).*

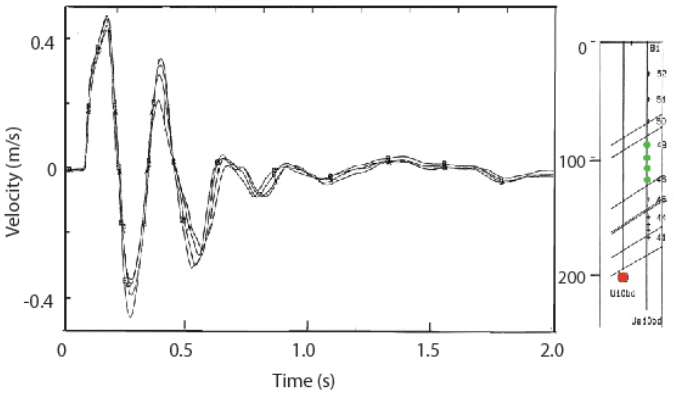

***Figure 6**: Velocity time histories for four sensors (green) within the quasi-elastic zone of event PERA (red).*

Discussion and Conclusions

The vast amount of ground motion data recorded during the U.S. underground nuclear testing program provides unique insights into material response and wave propagation and attenuation within the near-source regions of seismic events as large as ~M6. These regions extend from the zone of intense macroscopic damage and highly non-linear behavior under high strain and strain rate loading close to the detonation point through

the transition to elastic wave propagation to the response of the free-surface, where material response can again becomes non-linear owing to spalling under tensional failure. Much of this data set, together with instrument calibrations and material properties, is available to researchers through the archiving efforts at LLNL, LANL and SNL.

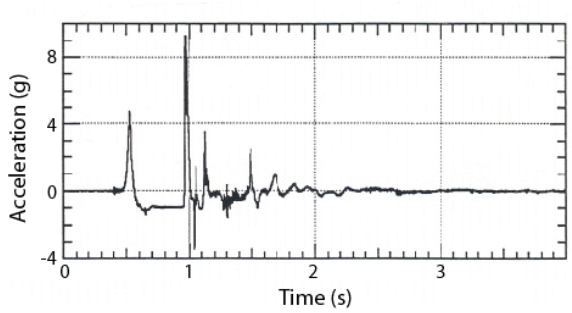

***Figure 7**: Ground surface vertical acceleration time history at a slant range of 1.1 km from event MOLBO.*

The data show that ground motions generated by nuclear explosions are severely attenuated by highly non-linear damage mechanisms and yielding within a few hundred meters of the detonation point, but that the transition to quasi-elastic and elastic material response is sharp and well defined. Although explosions and earthquakes are quite different seismic sources, this behavior is likely analogous to damage and non-linear attenuation mechanisms within a fault zone resulting from dynamic shear rupture that inherently limit the energy that can be propagated elastically. Although shear failure is one of the primary damage mechanisms close to an explosion source, pore compaction under a purely compressive stress regime also predominates in many of the materials at NTS. Therefore, the extent to which explosion data can be applied to the earthquake source should be one of the first topics of research in this field. Irrespective of the loading and damage mechanisms themselves, the ground motion and other data available for NTS have the potential to provide significant insights into the properties of materials analogous to the tuffs at the repository level at Yucca Mountain at high strains and strain rates. One way to achieve this is to use the recorded data to constrain the parameters in dynamic models of wave propagation and damage from selected explosions. This was done extensively as part of the containment programs at the national laboratories, and the data continue to be used to constrain more sophisticated models of explosion effects (e.g. Antoun et al., 1999).

Acknowledgments

I would like to thank Jeff Wagoner and John Rambo for detective work and assembling the spread sheets, and the LLNL D&NT Containment program for support. This work was performed under the auspices of the U.S. Department of Energy by University of California, Lawrence Livermore National Laboratory under Contract W-7405-Eng-48.

References

Antoun, T.H., O.Y. Vorobiev, I.N. Lomov, and L.A. Glenn, Simulations of an underground explosion in granite, American Physical Society Proc. 11th Topical Conference on Shock Compression of Condensed Matter, Snowbird, Utah, Jun 27-Jul 2, 1999.

App, F.N., The NTS ground motion data base, LAUR-94-1557, Los Alamos National Laboratory, 5 p., 1994.

Terhune, R.W., and M. Heusinkveld, Analysis of near field ground motion from nuclear detonations in high porosity media, Proc. Second Symposium on Containment of Underground Nuclear Explosions, Albuquerque, NM, Aug 2-3, 1983, v. 2, 123-164, 1983.

U.S. Department of Energy, United States nuclear tests, July 1945 through September 1 1992, DOE/NV--209-REV 15, 162 p., 2000.